RESEARCH ARTICLE SUMMARY

PLANT SCIENCE

Enhanced sustainable green revolution yield via nitrogen-responsive chromatin modulation in rice

Kun Wu*, Shuansuo Wang*, Wenzhen Song, Jianqing Zhang, Yun Wang, Qian Liu, Jianping Yu, Yafeng Ye, Shan Li, Jianfeng Chen, Ying Zhao, Jing Wang, Xiaokang Wu, Meiyue Wang, Yijing Zhang, Binmei Liu, Yuejin Wu, Nicholas P. Harberd†, Xiangdong Fu†

INTRODUCTION: The green revolution of the 1960s boosted cereal crop yields in part through widespread adoption of semi-dwarf plant varieties. The beneficial semi-dwarfism is respectively conferred in wheat and rice green revolution varieties by mutant *Reduced height-1* (*Rht-1*) and *semi-dwarf1* (*sd1*) alleles. These alleles cause accumulation of growth-repressing DELLA proteins, the normal forms of which are characterized by the presence of an Asp-Glu-Leu-Leu-Ala amino acid motif. Resultant semi-dwarf plants resisted lodging but required high nitrogen fertilizer inputs to maximize yield. Normally, gibberellin promotes growth by stimulating DELLA degradation as regulated by the gibberellin receptor GID1 (GIBBERELLIN INSENSITIVE DWARF1), the F-box protein GID2 (GIBBERELLIN INSENSITIVE DWARF2), and the SCF (Skp, Cullin, F-box–containing) ubiquitin ligase complex. Nitrogen fertilization–induced increase in grain yield is determined by the integration of three components (tiller number, grain number, and grain weight), but exogenous application of gibberellin reduces tiller number in rice. Here, we asked how nitrogen fertilization affects the gibberellin signaling that regulates rice tillering. Nitrogen fertilization promotes crop yield, but overuse in agriculture degrades the environment. A future of sustainable agriculture demands improved nitrogen use efficiency.

RATIONALE: Increased tillering, nitrogen fertilization, and high-density planting all contribute to the high yield typical of green revolution rice varieties. Increases in tiller number despite reduced nitrogen fertilization could help to sustain yield while reducing the environmental impact of agriculture. To investigate the effect of gibberellin on nitrogen-promoted rice tillering, we used genetic screening to identify a mutation in the *ngr5* (*nitrogen-mediated tiller growth response 5*) gene. Plants carrying the *ngr5* mutant displayed fewer tillers; tiller number was insensitive to nitrogen supply. Further genetic and biochemical studies defined the mechanisms underlying the interaction between nitrogen- and gibberellin-mediated effects on tiller number.

RESULTS: We found that increased nitrogen supply enhanced transcription and abundance of the rice APETALA2-domain transcription factor encoded by an *NGR5* (*NITROGEN-MEDIATED TILLER GROWTH RESPONSE 5*) allele. NGR5 interacts with a component of the polycomb repressive complex 2 (PRC2) and alters the genome-wide histone H3 lysine 27 trimethylation (H3K27me3) pattern response to changes in nitrogen availability. The extent of this alteration was reduced in *ngr5* plants or by gibberellin treatment. RNA sequencing and chromatin immunoprecipitation (ChIP)–polymerase chain reaction analysis showed that an increase in nitrogen supply reduced the abundance of mRNAs specified by strigolactone signaling and other branching-inhibitory genes [such as *Dwarf14* (*D14*) and *squamosa promoter binding protein-like–14* (*OsSPL14*)] in a dosage-dependent manner. Lack of *D14* or *OsSPL14* function was epistatic to *ngr5* in regulating rice tillering. We next found that the DELLA-mediated enhancement of nitrogen-induced tiller number, typical of green revolution rice varieties, was abolished in plants with the *ngr5* mutation.

ON OUR WEBSITE

Read the full article at http://dx.doi.org/10.1126/science.aaz2046

These observations suggest that NGR5-driven recruitment of PRC2 promotes repressive H3K27me3 modification of target branching-inhibitory genes, thus causing an increase in tiller number. On the other hand, a nitrogen-induced NGR5-dependent increase in tiller number is enhanced in green revolution rice varieties, and this effect is inhibited by gibberellin treatment. Although NGR5 abundance is negatively associated with gibberellin amount, gibberellin-promoted destabilization of NGR5 is neither dependent on nor downstream of gibberellin-induced DELLA destruction. Moreover, NGR5 interacts with the gibberellin receptor GID1 and DELLA proteins; this suggests that gibberellin-promoted proteasomal destruction of NGR5 is not due to gibberellin-promoted destruction of DELLAs, but is due to a gibberellin-potentiated interaction of NGR5-GID1, leading to polyubiquitination of NGR5 and subsequent destruction in the proteasome. Accumulation of DELLA proteins competitively inhibited the GID1-NGR5 interaction, thus stabilizing NGR5 by reducing its gibberellin-GID1–mediated destruction.

CONCLUSION: We conclude that nitrogen fertilization alters genome-wide reprogramming of H3K27me3 methylation via NGR5-dependent recruitment of PRC2. In rice, methylation represses genes that inhibit tillering and consequently promotes an increase in tiller number. NGR5 is a target of gibberellin-GID1–promoted proteasomal destruction. Modulation of competitive interactions among NGR5, DELLA proteins, and GID1 enables enhanced grain yield in elite rice varieties despite reduced nitrogen fertilizer inputs. Such shifts in yield and input use could promote agricultural sustainability and food security. ■

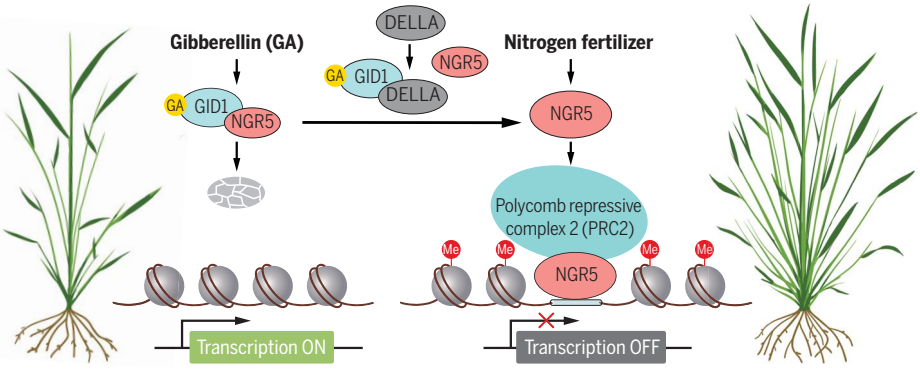

Nitrogen-responsive chromatin modulation enhances rice tillering. The rice transcription factor NGR5 facilitates nitrogen-dependent recruitment of PRC2 to repress expression of shoot branching-inhibitory genes, thus promoting tillering in response to increasing nitrogen supply. NGR5 interacts with the gibberellin receptor GID1 and with growth-repressing DELLA proteins. DELLA accumulation competitively inhibits the GID1-NGR5 interaction, thus stabilizing NGR5 by reducing gibberellin- and GID1-promoted proteasomal destruction.

The list of author affiliations is available in the full article online.
*These authors contributed equally to this work.
†Corresponding author. Email: nicholas.harberd@plants.ox.ac.uk (N.P.H.); xdfu@genetics.ac.cn (X.F.)
Cite this article as K. Wu *et al.*, *Science* **367**, eaaz2046 (2020). DOI: 10.1126/science.aaz2046

RESEARCH ARTICLE

PLANT SCIENCE

Enhanced sustainable green revolution yield via nitrogen-responsive chromatin modulation in rice

Kun Wu[1]*, Shuansuo Wang[1]*, Wenzhen Song[1,2], Jianqing Zhang[1,2], Yun Wang[1,2], Qian Liu[1], Jianping Yu[1], Yafeng Ye[1,3], Shan Li[1,2], Jianfeng Chen[1,2], Ying Zhao[1,2], Jing Wang[1,2], Xiaokang Wu[1,2], Meiyue Wang[4], Yijing Zhang[4], Binmei Liu[3], Yuejin Wu[3], Nicholas P. Harberd[5]†, Xiangdong Fu[1,2]†

Because environmentally degrading inorganic fertilizer use underlies current worldwide cereal yields, future agricultural sustainability demands enhanced nitrogen use efficiency. We found that genome-wide promotion of histone H3 lysine 27 trimethylation (H3K27me3) enables nitrogen-induced stimulation of rice tillering: APETALA2-domain transcription factor NGR5 (NITROGEN-MEDIATED TILLER GROWTH RESPONSE 5) facilitates nitrogen-dependent recruitment of polycomb repressive complex 2 to repress branching-inhibitory genes via H3K27me3 modification. NGR5 is a target of gibberellin receptor GIBBERELLIN INSENSITIVE DWARF1 (GID1)–promoted proteasomal destruction. DELLA proteins (characterized by the presence of a conserved aspartate-glutamate-leucine-leucine-alanine motif) competitively inhibit the GID1-NGR5 interaction and explain increased tillering of green revolution varieties. Increased NGR5 activity consequently uncouples tillering from nitrogen regulation, boosting rice yield at low nitrogen fertilization levels. NGR5 thus enables enhanced nitrogen use efficiency for improved future agricultural sustainability and food security.

The agricultural green revolution of the 1960s enhanced cereal crop yields, fed a growing world population, and was in part due to increased cultivation of semi-dwarf green revolution varieties (*1*–*4*). The beneficial semi-dwarfism is conferred by mutant alleles at the wheat *Reduced height-1* (*Rht-1*) (*5*, *6*) and rice *Semi-dwarf1* (*SD1*) (*7*, *8*) loci that enhance the activity of growth-repressing DELLA proteins (DELLAs). Normally, the phytohormone gibberellin stimulates the destruction of DELLAs (*9*, *10*), thus promoting plant growth. However, the mutant wheat DELLA protein Rht-1 likely resists gibberellin-stimulated destruction (*5*), whereas the rice *sd1* allele reduces gibberellin abundance (*11*, *12*) and increases accumulation of the rice DELLA protein SLR1 (SLENDER RICE1) (*13*). The result is plants that are shorter than normal, which, because they are shorter, are more resistant to lodging (the flattening of plants by wind and rain) (*4*). However, green revolution rice varieties require a high-nitrogen fertilizer supply to achieve maximum yield potential, and the drive toward increased agricultural sustainability necessitates reduced nitrogen fertilizer use (*13*). Grain yield is the sum of the multiplicative integration of three major components [tiller numbers per plant, grain numbers per panicle, and 1000-grain weight (*14*)], and an increased tillering ability in high-density planting conditions contributes to the high-yield properties of green revolution rice varieties (*1*, *15*). Further increase in tiller (lateral branch) numbers at low nitrogen supply is therefore important for future agricultural sustainability and is a key cereal breeding goal. Here, we first define the mechanisms underlying the promotive effects of nitrogen on tiller bud outgrowth. We then show how genetic modulation of these mechanisms can enable increased grain yield of green revolution varieties despite reduced nitrogen input, thus advancing agricultural sustainability.

Nitrogen promotes rice tillering via NGR5

We found that the tiller number per plant of *indica* rice variety Nanjing6 (NJ6) increased with increasing nitrogen supply (Fig. 1A). Additional effects of increased nitrogen on NJ6 included increases in grain number (per panicle) and yield (per plant) (*13*) (fig. S1, A to C). NJ6-*sd1* (a NJ6 isogenic line containing the *sd1* allele) also displayed nitrogen-dependent tiller number increases: increased tiller numbers per plant under different nitrogen fertilization levels, with tiller numbers being consistently higher in NJ6-*sd1* than in NJ6 (Fig. 1A). The *Rht-B1b* (formerly termed *Rht-1*) allele conferred similar properties on wheat

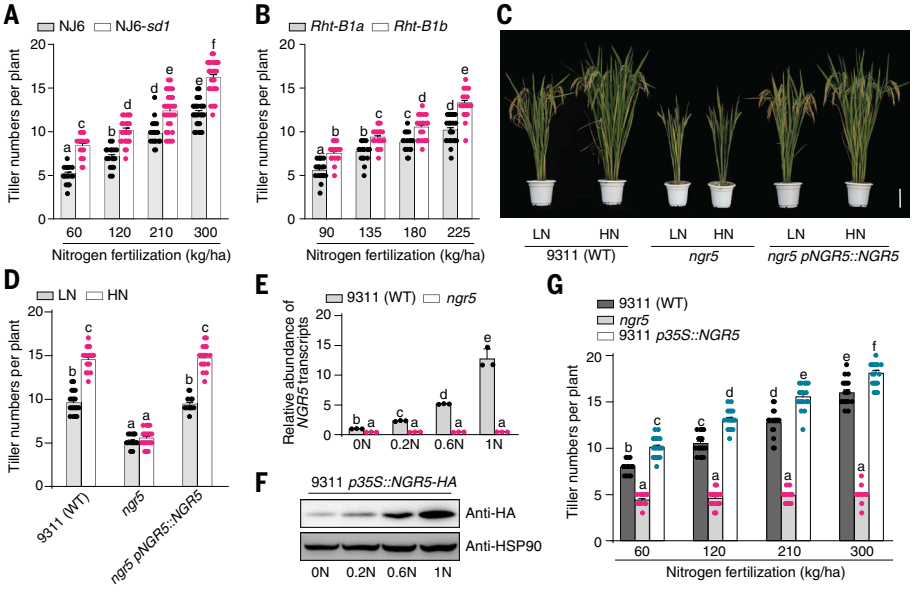

Fig. 1. NGR5 mediates nitrogen-dependent promotion of tillering. (**A** and **B**) Tiller numbers of field-grown rice and wheat plants in response to nitrogen supply. (A) NJ6 versus NJ6-*sd1*. (B) *Rht-B1a* versus *Rht-B1b*. Data are means ± SE (n = 30). (**C**) Mature plants grown in low (90 kg/ha; LN) versus high (180 kg/ha; HN) nitrogen supply. Scale bar, 20 cm. (**D**) Tiller numbers at LN (90 kg/ha) versus HN (180 kg/ha). Data are means ± SE (n = 20). (**E**) *NGR5* mRNA abundance in tiller buds. Three-week-old plants were grown hydroponically with varying nitrogen supply (0.2N, 0.25 mM NH_4NO_3; 0.6N, 0.75 mM NH_4NO_3; 1N, 1.25 mM NH_4NO_3), mRNA abundance values are relative to that of 0N (set to 1). Data are means ± SE (n = 3). (**F**) Accumulation of NGR5-HA in tiller buds of 3-week-old plants [as shown in (E)]. Heat shock protein 90 (HSP90) serves as loading control. (**G**) Tiller numbers of field-grown rice plants under increasing nitrogen supply. Data are means ± SE (n = 20). In (A), (B), (D), (E), and (G), different letters denote significant differences (P < 0.05, Duncan multiple-range test).

[1]State Key Laboratory of Plant Cell and Chromosome Engineering, Institute of Genetics and Developmental Biology, Innovation Academy for Seed Design, Chinese Academy of Sciences, Beijing 100101, China. [2]College of Life Sciences, University of Chinese Academy of Sciences, Beijing 100049, China. [3]Key Laboratory of High Magnetic Field and Ion Beam Physical Biology, Hefei Institutes of Physical Science, Chinese Academy of Sciences, Hefei, Anhui 230031, China. [4]National Key Laboratory of Plant Molecular Genetics, CAS Center for Excellence in Molecular Plant Sciences, Shanghai Institute of Plant Physiology and Ecology, Shanghai Institutes for Biological Sciences, Chinese Academy of Sciences, Shanghai 200032, China. [5]Department of Plant Sciences, University of Oxford, Oxford OX1 3RB, UK.
*These authors contributed equally to this work.
†Corresponding author. Email: nicholas.harberd@plants.ox.ac.uk (N.P.H.); xdfu@genetics.ac.cn (X.F.)

(versus the *Rht-B1a* control allele; Fig. 1B and fig. S1, D to F). In contrast, either exogenous gibberellin treatment or overexpression of the rice gibberellin receptor GID1 (*16*) inhibited nitrogen-promoted tillering (fig. S2). Thus, the enhanced DELLA function typical of green revolution varieties increases nitrogen-induced promotion of tiller number. Further analysis showed that nitrogen-induced increases in tiller number in the elite *sd1*-containing *indica* rice variety 9311 (fig. S3, A and B) were not due to nitrogen-responsive increases in numbers of lateral buds, but rather to increased numbers of buds initiating outgrowth and tiller branch extension (*17*) (fig. S3, C to E).

We next screened an ethyl methane sulfonate (EMS)–mutagenized 9311 population for mutants displaying an altered tiller number nitrogen response. Among such mutants, *ngr5* (*nitrogen-mediated tiller growth response 5*) displayed a reduced tiller number that was insensitive to changes in nitrogen supply (Fig. 1, C and D). Map-based cloning (fig. S4, A and B) and genetic complementation (Fig. 1, C and D, and fig. S4, C and D) revealed the *NGR5* allele to encode an APETALA2 (AP2)–domain transcription factor [NGR5, previously known as SMOS1 (SMALL ORGAN SIZE1) and RLA1 (REDUCED LEAF ANGLE1)] (*18*–*20*), thus identifying an unknown function for NGR5 in nitrogen-responsive tillering regulation. The *ngr5* allele carries a G → A nucleotide substitution conferring a Gly → Arg mutant protein (fig. S4B), which fails to complement *ngr5* phenotypes (fig. S4, C to F). In addition to its effect on tiller number (Fig. 1, C and D, and fig. S4D), *NGR5* is required for nitrogen-induced promotion of panicle branching and grain number (fig. S4, E and F). Accordingly, whereas 9311 grain yield per plot increased progressively with increasing nitrogen supply (*13*), this effect was abolished in *ngr5* plants (fig. S4G). Further analysis showed that lack of NGR5 (in *ngr5* plants) had no effect on the formation of tiller buds (lateral bud initials; fig. S3C) but reduced the number of buds initiating lateral outgrowth and tiller branch extension (fig. S3, D and E), thus confirming that nitrogen-responsive regulation of tillering is dependent on *NGR5*.

We next found that an increasing nitrogen supply increased NGR5 abundance at both mRNA and protein levels (Fig. 1, E and F). First, increasing nitrogen supply increased *NGR5* mRNA abundance, and this effect was abolished in *ngr5* plants (Fig. 1E). Second, although nitrogen supply had no effect on *NGR5-HA* (hemagglutinin-tagged fusion gene) mRNA abundance in plants transgenically expressing *p35S::NGR5-HA* (fig. S5), accumulation of NGR5-HA fusion protein increased with increasing nitrogen supply (Fig. 1F). Furthermore, NGR5 positively regulated tillering over a wide expression range, because the *p35S::NGR5* transgene increased 9311 tiller number (thus mimicking the effect of increasing nitrogen supply on tillering capacity; Fig. 1G). We conclude that nitrogen promotes increased NGR5 abundance, which in turn promotes tiller bud outgrowth. In addition, because *ngr5* suppressed the *sd1*-conferred tillering phenotype of 9311 (Fig. 1D), NGR5 is necessary for the DELLA-promoted increase in tiller number characteristic of green revolution varieties.

NGR5 represses branching-inhibitory genes

RNA sequencing (RNA-seq) analysis next revealed that lack of *NGR5* causes genome-wide change in mRNA abundance, with multiple differentially expressed genes displaying an increase in mRNA abundance in *ngr5* (fig. S6A). Further gene set enrichment analysis revealed a correlation between genes up-regulated in *ngr5* and the set of H3K27me3 (histone H3 lysine 27 trimethylation)–marked genes already known to be normally repressed by histone modification (fig. S6B), with H3K27me3 marks occurring at both TSS (transcription start site) and gene body regions of *ngr5*–up-regulated genes (fig. S6C). These results suggest that NGR5 may be involved in PRC2 (polycomb repressive complex 2)–mediated epigenetic repression. Among genes up-regulated in *ngr5* (table S1), we identified *D14* [*Dwarf14*, encoding the receptor for the phytohormone strigolactone (SL)] (*21*), *D3* [*Dwarf3*, encoding the F-box component of the Skp, Cullin, F-box–containing (SCF) ubiquitin ligase that targets the DWARF53 repressor of SL signaling for proteasomal destruction] (*22*–*24*), *OsTB1* (*TEOSINTE BRANCHED1*, encoding a TCP domain transcription factor) (*25*), and *OsSPL14* (*squamosa promoter binding protein-like–14*, encoding an SBP-domain transcription factor) (*26*, *27*) genes, all of which are already known to inhibit lateral branching and tiller number. Quantitative real-time polymerase chain reaction (qRT-PCR) analysis showed that high nitrogen supply reduced the abundances of mRNAs specified by these shoot branching-inhibitory genes, and this effect was abolished by lack of *NGR5* function (in *ngr5*; fig. S6D). In addition, we found that lack of *D14* or *OsSPL14* function (conferred by *d14* or *osspl14* alleles) (*28*, *29*) is epistatic to *ngr5* in regulating lateral branching (fig. S7). Thus, *D14* and *OsSPL14* function downstream of *NGR5*, and NGR5 mediates nitrogen-promoted increase in tiller number by repressing the inhibitory functions of *D14* and *OsSPL14* (and likely of other) branching-regulatory genes.

Chromatin immunoprecipitation–PCR (ChIP-PCR) experiments revealed binding of NGR5-HA to gene body and promoter regions of *D14* and *OsSPL14* [fig. S6E; confirmed in EMSA (electrophoretic mobility shift assays), fig. S6F]. Furthermore, the extent and effect of binding on NGR5-target gene repression correlated with increasing nitrogen supply (fig. S6, G and H). *D14* mRNA abundance decreased with increasing nitrogen supply in *NGR5* (but not in *ngr5*; fig. S6G), and the extent of NGR5 binding and the level of H3K27me3 modification at *D14* were correspondingly increased in a nitrogen-dependent manner (but not in *ngr5*; fig. S6G). Similar effects were observed for *OsSPL14* (fig. S6H), which suggests that NGR5 promotes tillering in response to increasing nitrogen supply by binding to target branching-inhibitory genes, thus causing their repression through regulation of H3K27me3 modification.

NGR5 recruits PRC2 for H3K27me3 deposition

To determine how NGR5 regulates nitrogen-promoted H3K27me3 modification, we first performed a yeast two-hybrid screen for NGR5 interactors, identifying LC2 (leaf inclination2, a component of the PRC2 complex) (*30*) among many others (table S2). NGR5-LC2 interactions were confirmed in bimolecular fluorescence complementation (BiFC; Fig. 2A) and coimmunoprecipitation (Co-IP; Fig. 2B) experiments. Furthermore, a CRISPR/Cas9-generated *LC2* reduced-function allele (*lc2*; fig. S8A) was shown, like *ngr5*, to abolish nitrogen-promoted increase in tiller number (Fig. 2, C and D). *lc2* also suppressed the increased tiller number conferred by *p35S::NGR5* (Fig. 1G and Fig. 2, C and D), whereas lack of *D14* or *OsSPL14* function (conferred by *d14* or *osspl14*) was epistatic to *lc2* (fig. S9). Taken together, these results suggest that NGR5-dependent nitrogen-promoted increase in tiller number depends on LC2 (PRC2 complex) function. Because PRC2 regulates genome-wide patterns of H3K27me3 methylation, we next conducted genome-wide surveys of H3K27me3 methylation in response to varying nitrogen supply. Although increasing nitrogen supply altered the genome-wide H3K27me3 methylation pattern, the extent of this alteration was reduced in *ngr5* (Fig. 2E), which suggests that nitrogen-mediated genome-wide reprogramming of H3K27me3 methylation is NGR5-dependent.

We next performed ChIP-sequencing experiments and identified a total of 453 binding sites shared in common by NGR5 and LC2 (Fig. 2F and tables S3 and S4). Further analysis identified potential target-site recognition motifs shared by NGR5 and LC2 (Fig. 2, G and H), with a predominant shared GCCGCC motif being common in the gene body regions of both *ngr5*–up-regulated and nitrogen-induced genes (Fig. 2E). Accordingly, increasing nitrogen supply progressively reduced *D14* and *OsSPL14* mRNA abundance in wild-type plants, and these effects were abolished in *lc2* plants (Fig. 2, I and J, top), just as they were in *ngr5* plants (fig. S6, G and H). Furthermore, increasing nitrogen

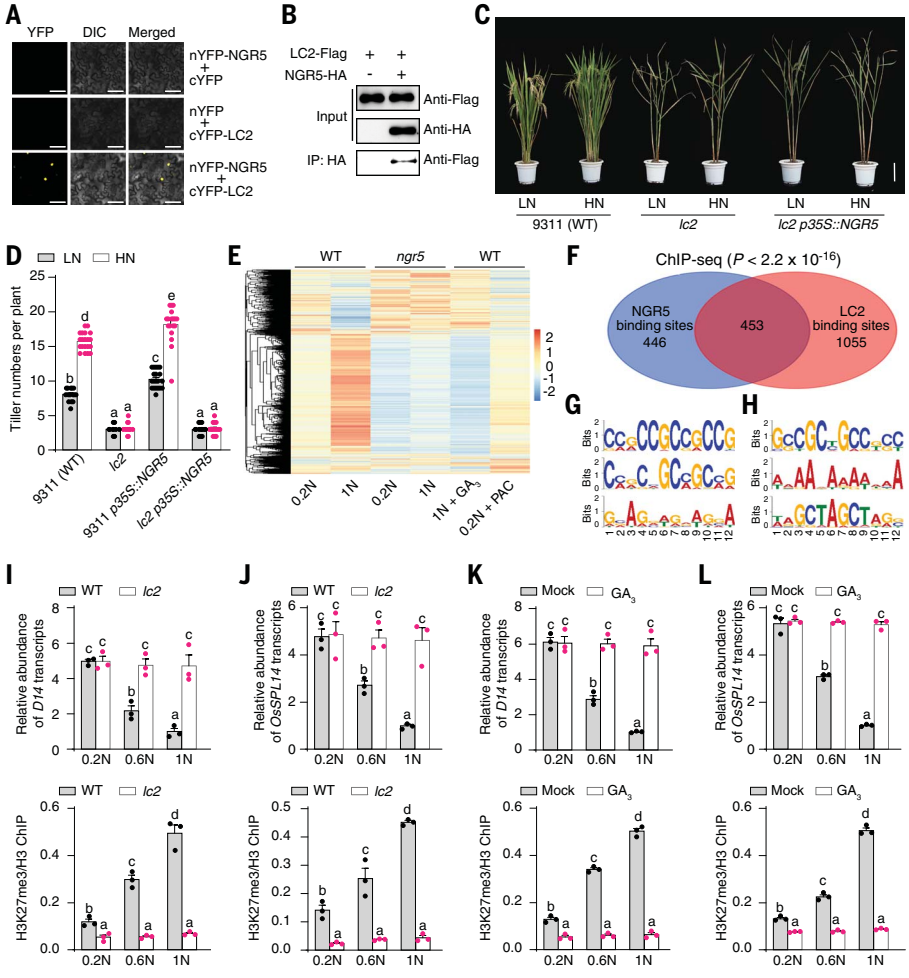

Fig. 2. Nitrogen regulates tillering via H3K27me3 reprogramming. (**A**) BiFC assays. Scale bar, 60 μm. (**B**) Co-IP assays. (**C**) Mature plants grown in low (90 kg/ha; LN) versus high (180 kg/ha; HN) nitrogen supply. Scale bar, 20 cm. (**D**) Tiller number. Data are means ± SE (n = 20). (**E**) Genome-wide surveys of H3K27me3 enrichment density. Each peak was normalized to zero mean and unit of energy (z-score). (**F**) Overlap of H3K27me3 ChIP-seq peaks. (**G** and **H**) Sequence motifs enriched during ChIP-seq with NGR5-HA (G) and LC2-HA (H). (**I** and **J**) Comparisons of mRNA abundance and H3K27me3 modification of *D14* (I) and *OsSPL14* (J) between 9311 [wild type (WT)] and *lc2*. (**K** and **L**) Transcript abundance and H3K27me3 modification of *D14* (K) and *OsSPL14* (L) in 9311 with or without 100 μM GA_3 treatment. RT-PCR and ChIP experiments [(F), (I) to (L)] were performed using tiller buds of 3-week-old plants grown in increasing nitrogen supply (0.2N, 0.25 mM NH_4NO_3; 0.6N, 0.75 mM NH_4NO_3; 1N, 1.25 mM NH_4NO_3); mRNA abundance values are relative to that of WT in 1N (set to 1). Data in (I) to (L) are means ± SE (n = 3). In (D) and (I) to (L), different letters denote significant differences (P < 0.05, Duncan multiple range test).

supply progressively increased H3K27me3 modification of both *D14* and *OsSPL14* in wild-type plants, and these effects were also abolished in *lc2* plants (Fig. 2, I and J, bottom). Taken together, these observations suggest that NGR5-driven recruitment of the PRC2 complex (of which LC2 is a component) to *D14* and *OsSPL14* results in repressive H3K27me3 modification of these genes in response to increased nitrogen supply, thereby promoting bud outgrowth and increasing tiller number.

NGR5 is a target of gibberellin receptor GID1

As shown above, nitrogen-induced increase in tiller number was enhanced in green revolution varieties (Fig. 1, A and B), and this effect was inhibited by exogenous gibberellin treatment (fig. S2A). Analysis of both RNA-seq and ChIP sequencing revealed multiple common gene targets to be co-regulated by NGR5 and gibberellin treatment (tables S5 and S6). Furthermore, gibberellin treatment altered the change in genome-wide H3K27me3 modification pattern due to increasing nitrogen supply in a manner similar to the alteration conferred by *ngr5*, whereas a partially restored H3K27me3 modification pattern was induced by treatment with paclobutrazol (PAC, an inhibitor of gibberellin biosynthesis; Fig. 2E). In addition, gibberellic acid (GA_3), like *ngr5* and *lc2*, inhibited the nitrogen-dependent increase in H3K27me3 modification and consequent repression of expression of shoot branching inhibitor genes such as *D14* (Fig. 2K) and *OsSPL14* (Fig. 2L). These observations suggest the existence of a mechanistic link between nitrogen- and gibberellin-mediated effects on tiller number.

In canonical gibberellin signaling, gibberellin binds its receptor GID1, thus recruiting DELLAs for polyubiquitination by the F-box protein GIBBERELLIN INSENSITIVE DWARF2 (GID2) and the Skp, Cullin, F-box–containing (SCF) ubiquitin ligase complex (SCF^{GID2}) and subsequent destruction in the 26*S* proteasome, thus promoting plant growth (*9*, *10*, *16*, *31*–*34*). We next found that reduced GID1 function in a NJ6-*gid1-10* mutant (*gid1* loss-of-function mutant; fig. S8B) led to an increased tiller number above that of NJ6 controls in both high and low nitrogen supply (similar to NJ6-*sd1*; Fig. 3, A and B). Conversely, transgenic NJ6-*sd1* plants overexpressing *GID1* under the control of the cauliflower mosaic virus (CaMV) 35*S* promoter exhibited nitrogen-insensitive responses, with lower tiller number than in nontransgenic controls (Fig. 3B). Although gibberellin repressed tiller number in both NJ6 and NJ6-*sd1* plants, it had no effect on tiller number in NJ6-*gid1-10* or NJ6-*sd1-ngr5* plants, nor in NJ6-*sd1* plants overexpressing *GID1* (Fig. 3B). Furthermore, either gibberellin-induced inhibition or GID1-mediated repression of tillering mimicked the effect of *ngr5* (Fig. 3B). These results suggest that gibberellin-GID1–mediated repression of tiller number is dependent on the nitrogen-regulated function of NGR5.

We next found that NGR5 abundance is negatively associated with gibberellin level: NGR5-HA accumulation was increased in relatively gibberellin-deficient NJ6-*sd1* plants (versus NJ6), whereas it was reduced by exogenous gibberellin treatment (Fig. 3C). Conversely, a gibberellin-mediated decrease in NGR5-HA abundance was inhibited by treatment with the proteasome inhibitor MG132 (carbobenzoxy-Leu-Leu-leucinal), such that NGR5-HA accumulation was increased above that of NJ6-*sd1* plants (Fig. 3C). Accordingly, Western blot analysis detected the accumulation of polyubiquitinated NGR5-HA in the presence of MG132 (Fig. 3D), which suggests that gibberellin promotes polyubiquitination and subsequent proteolysis of NGR5 in the 26*S* proteasome. In addition, gibberellin-induced degradation of NGR5-HA was inhibited in the NJ6-*gid1-10* mutant (Fig. 3E), indicating that gibberellin-induced promotion of NGR5 polyubiquitination and proteasome destruction is dependent on the *GID1* function.

Gibberellin responses are conventionally considered to be activated by GID1-mediated destruction of DELLAs (*9*, *10*). However, we found that gibberellin-mediated degradation of NGR5-HA occurs either in the absence of

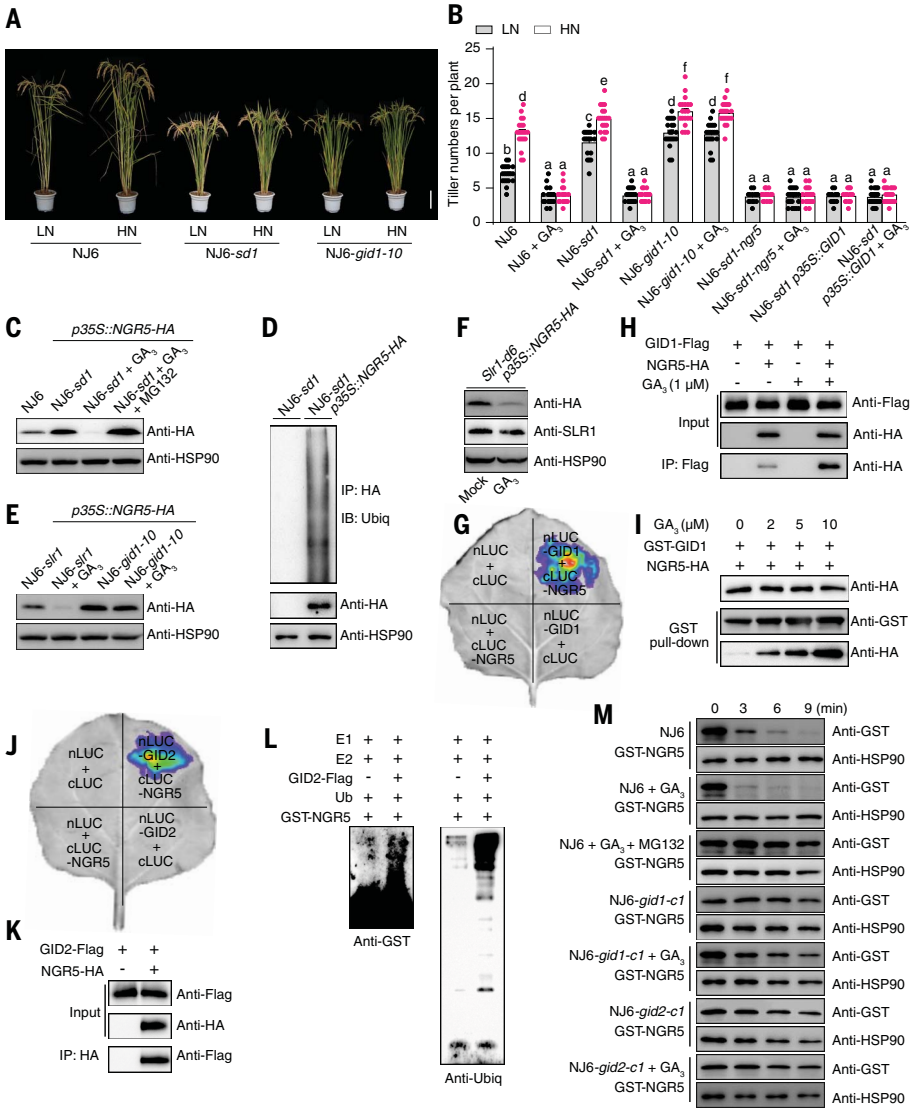

Fig. 3. Gibberellin-GID1-SCF^{GID2} targets NGR5 for destruction. (**A**) Mature plants grown in low (90 kg/ha; LN) versus high (180 kg/ha; HN) nitrogen supply. Scale bar, 20 cm. (**B**) Tiller number. Data are means ± SE (n = 20). (**C**) Immunodetection of NGR5-HA. (**D**) Immunodetection of poly-ubiquitinated NGR5-HA. (**E**) Accumulation of NGR5-HA. (**F**) Effects of gibberellin on NGR5-HA and SLR1 accumulation. In (C) to (F), total protein was extracted from tiller buds of 3-week-old plants treated for 4 hours with 1 μM GA_3 and/or 100 μM MG132; HSP90 serves as loading control. (**G** and **J**) SFLC assays. nLUC-tagged GID1 (G) or nLUC-tagged GID2 (J) was co-transformed into tobacco leaves along with cLUC-targeted NGR5. (**H** and **K**) Co-IP assays. Flag-tagged GID1 (H) or Flag-tagged GID2 (K) was co-transformed into rice protoplasts along with HA-targeted NGR5. (**I**) Pull-down assays. (**L**) In vitro ubiquitination assay. The immunoprecipitated GID2-Flag proteins transiently expressed in rice protoplasts were used in an in vitro ubiquitination reaction in the presence of E1, E2 (UbcH5B), His-Ub, and GST-NGR5. (**M**) Gibberellin-GID1-SCF^{GID2} destabilizes GST-NGR5. Lysates from NJ6, NJ6-*gid1-c1*, and NJ6-*gid2-c1* plants were co-incubated with GST-NGR5 in the presence or absence of 100 μM GA_3 and 100 μM MG132. The lysates were harvested at various incubation times and immunoblotted to assess the accumulation of NGR5 and HSP90.

DELLAs in a loss-of-function *slr1* mutant (Fig. 3E) (*11*) or in the presence of the high-level DELLA accumulation conferred by the *Slr1-d6* gain-of-function mutation (Fig. 3F) (*35*). Although the mutant SLR1 DELLA encoded by *Slr1-d6* was relatively resistant to gibberellin-mediated destruction, NGR5-HA was still destabilized by exogenous gibberellin treatment (Fig. 3F). Thus, gibberellin-promoted destabilization of NGR5, although dependent on GID1, is neither dependent on nor downstream of gibberellin-induced destruction of DELLAs. We therefore explored the possibility of an alternative, previously unknown, DELLA-independent mechanism whereby the SCF^{GID2} E3 ubiquitin ligase directly mediates gibberellin-promoted destruction of NGR5, finding that GID1 interacts directly with NGR5 [as assayed by both split firefly luciferase complementation (SFLC) and Co-IP; Fig. 3, G and H] and that the strength of this interaction is potentiated by increasing concentrations of gibberellin (Fig. 3, H and I). Thus, as with the DELLAs, gibberellin enhances the interaction between NGR5 and GID1, thereby identifying NGR5 as a potential alternative substrate for GID1-promoted polyubiquitination.

Although NGR5 lacks the specific DELLA motif that enables the GID1-DELLA interaction (*33*, *34*), we found a motif within the AP2-R2 (repeated units 2) (*18*) domain of NGR5 to enable the GID1-NGR5 interaction (fig. S10). Furthermore, NGR5 also interacted with the GID2 F-box component of the SCF^{GID2} E3 ubiquitin ligase that normally targets SLR1 for destruction in the 26*S* proteasome (Fig. 3, J and K). Accordingly, an in vitro ubiquitination assay showed that GST (glutathione *S*-transferase)–NGR5 fusion protein is polyubiquitinated by GID2-Flag (Asp-Tyr-Lys-Asp-Asp-Asp-Asp-Lys peptide) fusion protein in the presence of ubiquitin-activating enzyme E1, ubiquitin-conjugating enzyme E2, and ubiquitin, but not in the absence of GID2-Flag (Fig. 3L), which suggests that NGR5 is a substrate of the SCF^{GID2} E3 ubiquitin ligase. Additional time-course experiments showed that gibberellin promotes the progressive degradation of GST-NGR5 but that this degradation is inhibited both by MG132 and in *gid1-c1*, a CRISPR/Cas9-generated *GID1* loss-of-function mutant (Fig. 3M and fig. S8B). Finally, lack of GID2 function (in a *gid2-c1* mutant; fig. S8C) also inhibits gibberellin-mediated degradation of GST-NGR5 (Fig. 3M). We conclude that the gibberellin-mediated regulation of NGR5 is not due to gibberellin-promoted destruction of DELLAs, but is due to a previously unknown direct and gibberellin-potentiated interaction of NGR5-GID1, leading to polyubiquitination of NGR5 by the SCF^{GID2} E3 ubiquitin ligase and subsequent destruction in the proteasome.

DELLA-NGR5 modulation of tiller N response

We next found that NGR5 interacts directly with SLR1 [in yeast two-hybrid screens (table S2) and in BiFC and Co-IP assays (fig. S11, A and B)]. Nonetheless, we additionally found that the LC2-NGR5 interaction is not inhibited by the presence of SLR1 (fig. S12), which suggests that the SLR1-NGR5 interaction does not directly interfere with the LC2-NGR5 interaction that determines NGR5 function. Further experiments showed that the LHR1 (leucine heptad repeat 1) motif of the DELLA protein is necessary for the NGR5-SLR1 interaction

(fig. S11C). Thus, in addition to both being substrates of gibberellin-GID1-SCF^{GID2}, SLR1 and NGR5 interact directly with one another. With the LHR1 motif being conserved in all the GRAS [derived from three initially identified members, GAI (gibberellin-insensitive), RGA (repressor of ga1-3), and SCARECROW] proteins, we next found that NGR5 interacts with two additional GRAS proteins [DWARF AND LOW-TILLERING (DLT) and MONOCULM1 (MOC1)] previously shown to regulate tiller number (*17*, *19*, *36*) (fig. S13A). The competitive nature of the SLR1-NGR5 relationship with respect to GID1 (and hence with respect to GID1-promoted destruction) (fig. S13B) caused accumulation of NGR5-HA (conferred by *p35S::NGR5-HA*) to further increase the accumulation of SLR1 in 9311 (fig. S13C).

We next determined whether competitive SLR1-NGR5-GID1 relationships also condition gibberellin and nitrogen effects on tiller number. As shown in Fig. 1B, the enhanced DELLA function conferred by the *Rht-B1b* allele results in increased tiller number. We therefore tested the possibility that the effect of *Rht-B1b* on tiller number might be due to differential effects on NGR5 stability. Accordingly, using FRET (Förster resonance energy transfer) analysis, we found that the extent of the interaction between GID1 and NGR5 is reduced by the presence of Rht-B1b (Fig. 4, A and B). We then confirmed the expectation that a reduced GID1-NGR5 interaction in the presence of Rht-B1b reduces the rate of proteasome-dependent GST-NGR5 destruction (Fig. 4C), and we found similar reductions to be conferred by accumulation of wild-type Rht-B1a or SLR1 proteins (Fig. 4, A to C). Further comparative studies showed His-NGR5 (His-tagged fusion protein) destruction to be more rapid than that of His-SLR1 (His-tagged fusion protein; Fig. 4D). Thus, although gibberellin-promoted NGR5 destruction was DELLA-independent (Fig. 3, E and F), competition between NGR5 and SLR1 for GID1 interaction reduced the extent of NGR5-GID1 interaction (fig. S13B). Moreover, the abundance of NGR5-GFP (green fluorescent protein) fusion protein (conferred by *p35S::NGR5-GFP*) was increased with PAC treatment but was reduced in response to combined gibberellin and PAC treatments (fig. S13, D and E). This is also consistent with the observations that *ngr5* exhibits a higher ratio of gibberellin-induced leaf sheath growth, whereas transgenic plants overexpressing *NGR5-HA* display reduced sensitivity to PAC treatment relative to wild-type controls (fig. S14). We conclude that the enhanced DELLA function characteristic of both wheat and rice green revolution varieties competitively inhibits the GID1-NGR5 interaction, thus stabilizing NGR5 by reducing gibberellin-GID1–mediated destruction.

To determine whether DELLA promotion of rice tillering is NGR5-dependent, we generated 9311 NILs (near-isogenic lines) carrying various combinations of different *SD1*, *GID1*, and *NGR5* alleles. Although the increased SLR1 accumulations in both 9311-*NGR5-gid1-10* and 9311-*NGR5-sd1* increased the tiller numbers of plants grown in either low or high nitrogen supply (versus 9311-*NGR5-SD1*), there was almost no difference in tiller number when 9311-*ngr5-sd1*, 9311-*ngr5-SD1*, and 9311-*ngr5-gid1-10* were compared (Fig. 4E). Thus, the DELLA-mediated enhancement of nitrogen-induced tiller number increase typical of green revolution rice varieties is dependent on NGR5 function. Accordingly, comparisons of NGR5-regulated mRNA abundance and H3K27me3 modification of branching-inhibitory *D14* (Fig. 4F) and *OsSPL14* (Fig. 4G) genes in 9311 (containing *sd1*) versus 9311-*SD1* revealed mRNA abundance and modification status at 0.6N in 9311-*SD1* to be roughly equivalent to that at 0.2N in

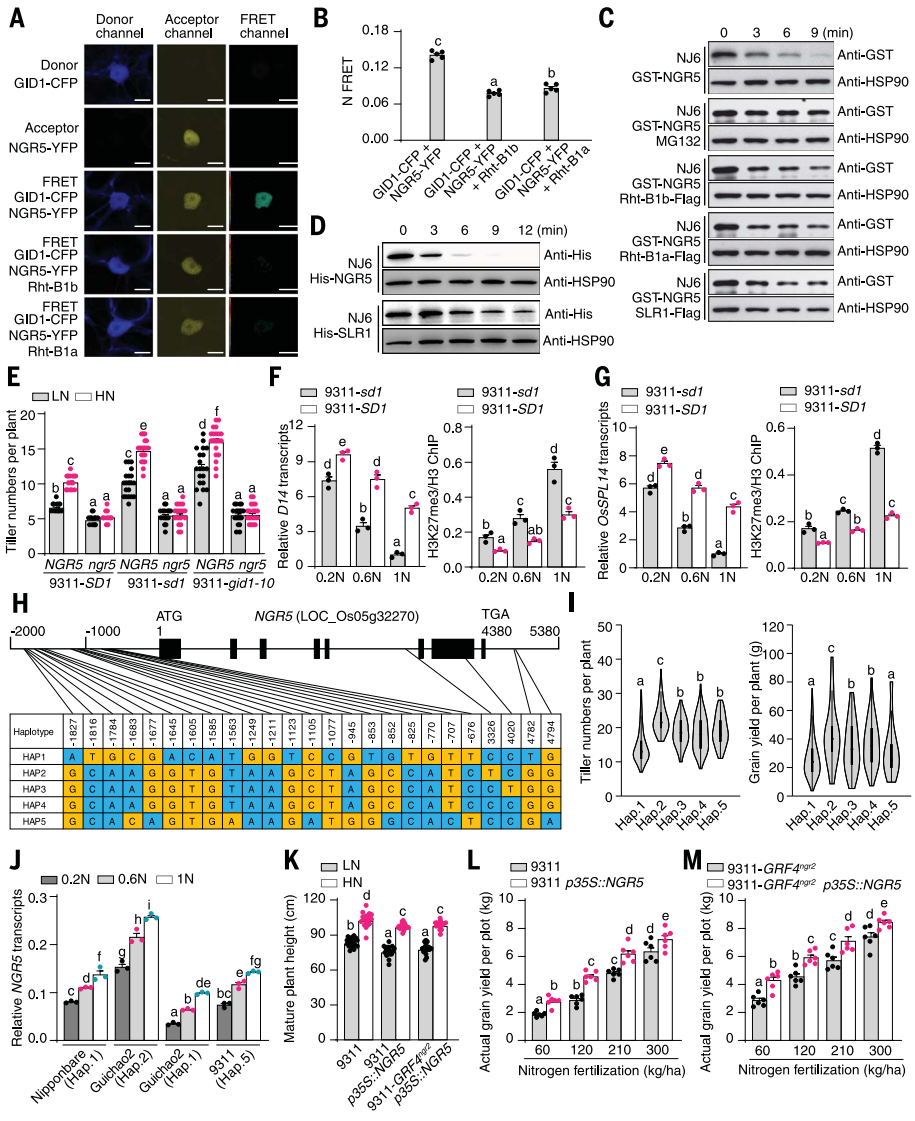

Fig. 4. Balanced DELLA-NGR5 interactions improve nitrogen use efficiency. (**A**) FRET images. Scale bars, 200 μm. (**B**) Mean N-FRET data for GID1-CFP and NGR5-YFP channels. Data are means ± SE (n = 5). (**C**) Time-course analysis of GST-NGR5 degradation. HSP90 serves as loading control. (**D**) Degradation rate of His-NGR5 and His-SLR1. (**E**) Tiller number. (**F** and **G**) Relative mRNA abundance and H3K27me3 modification of *D14* (F) and *OsSPL14* (G). Transcript abundance values are relative to that of 9311-*sd1* in 1N (set to 1). Data are means ± SE (n = 3). (**H**) Natural allelic variation at *NGR5*. (**I**) Tiller number and grain yield. Data are means ± SE (Hap.1, n = 305; Hap.2, n = 84; Hap.3, n = 62; Hap.4, n = 138; Hap.5, n = 97). (**J**) Relative mRNA abundance of *NGR5*. Abundance shown is relative to that of *OsActin1*. (**K**) Plant height. Data in (E) to (K) are means ± SE (n = 20). (**L** and **M**) Grain yield per plot. Data are means ± SE of six plots (each plot contained 220 plants) per line per nitrogen level. In (B), (E) to (G), and (I) to (M), different letters denote significant differences (P < 0.05, Duncan multiple range test).

9311-*sd1*. Thus, the enhanced DELLA function of *sd1* increases tiller number in response to nitrogen supply by increasing the stability of NGR5 (Fig. 3, C and E), which in turn inhibits the expression of shoot branching inhibitor genes, thereby promoting tiller number.

NGR5 improves yield and nitrogen use efficiency

We next determined whether an increase in NGR5 abundance beyond that seen in elite rice varieties (e.g., *sd1*-containing 9311) could further increase tiller number and yield in reduced nitrogen fertilizer inputs. First, we surveyed publicly available rice varietal genome sequence data for natural genetic variation at *NGR5* (*37*), distinguished five distinct haplotypes (Hap.1 to Hap.5; Fig. 4H), and found that Hap.2 was associated with increased *NGR5* mRNA abundances in both low and high nitrogen conditions (fig. S15), together with increases in tiller number and field-grown grain yield of 686 diverse Asian cultivated rice accessions (Fig. 4I). Further analysis showed that Hap.2-containing Guichao2 [Guichao2(Hap.2), one of the highest-yielding of *indica* varieties cultivated in China since the 1980s] displayed a greater *NGR5* mRNA abundance than did Guichao2(Hap.1) (a NIL carrying Hap.1 in the Guichao2 genetic background) and other lines (including Hap.5-containing 9311), even at low and moderate nitrogen supply (Fig. 4J). In addition, we showed that a transgenic mimic of Hap.2 (expression from a *p35S::NGR5* transgene) enhanced 9311 grain yield in a range of nitrogen supply conditions, without affecting the characteristic and beneficial semi-dwarfism of 9311 (Fig. 4, K and L); this suggests that breeding with Hap.2 is a feasible future strategy toward improving nitrogen use efficiency of the elite rice varieties. Finally, having recently shown that allelic variation at *GRF4* (encoding the rice GROWTH-REGULATING FACTOR 4 transcription factor) enhances grain yield and nitrogen use efficiency through coordinating effects on carbon and nitrogen metabolic regulation (*13*), we investigated the genetic interaction between *GRF4* and *NGR5*. We found that increased abundances of both *GRF4* and *NGR5* further enhanced 9311 yield and nitrogen use efficiency, particularly at relatively low levels of nitrogen supply (Fig. 4M).

We have shown that nitrogen determines genome-wide chromatin status (specific H3K27me3 histone modification) via NGR5-dependent recruitment of the polycomb complex PRC2 to target genes, among which are tiller branch-repressing genes. In consequence, repression of tiller outgrowth is reduced in increasing nitrogen supply, causing increased tillering. We have also shown that NGR5 is a non-DELLA target of gibberellin-GID1-SCF^{GID2}–mediated proteasomal destruction and that competitive NGR5-DELLA-GID1 interactions cause the NGR5-dependent yield-enhancing tillering increases typical of green revolution rice varieties. Because NGR5 is already known to be involved in the cross-talk between auxin and brassinosteroid signaling (*19*, *20*), our discoveries add to a growing understanding of how diverse modes of molecular and functional cross-talk between multiple phytohormonal signaling and fertilizer use responses function in the environmentally adaptive regulation of plant growth and development. Finally, we have shown that increasing NGR5 expression or activity provides a breeding strategy to reduce nitrogen fertilizer use while boosting grain yield above what is currently sustainably achievable.

Materials and methods

Plant materials and growth conditions

A nitrogen-insensitive rice mutant, designated *ngr5* (*nitrogen-mediated tiller growth response 5*), was isolated from the progeny of EMS-mutagenized *indica* cultivar 9311. NILs carrying allelic combinations of the *NGR5*, *SD1*, and *GID1* loci were obtained by backcrossing to recurrent parent 9311 (or NJ6) six times. Details of the germplasm used for the positional cloning and haplotype analysis are described in (*13*, *37*–*39*). Paddy-grown rice plants, including 686 diverse Asian cultivated rice accessions (*37*), were planted in rows 20 cm apart and raised in standard paddy conditions at two experimental stations, one in Lingshui (Hainan Province), the other in Hefei (Anhui Province).

Hydroponic culture conditions

Hydroponic culture conditions were as described (*13*). Rice seeds were surface-sterilized with 20% sodium hypochlorite solution for 30 min, then rinsed and soaked in water for 3 days to allow the seeds to germinate. Surface-sterilized seeds were then germinated in moist Perlite. Seven-day-old seedlings were transplanted to PVC pots containing 40 liters of nutrient solution (1.25 mM NH_4NO_3, 0.5 mM $NaH_2PO_4{\cdot}2H_2O$, 0.75 mM K_2SO_4, 1 mM $CaCl_2$, 1.667 mM $MgSO_4{\cdot}7H_2O$, 40 μM Fe-EDTA (Na), 19 μM H_3BO_3, 9.1 μM $MnSO_4{\cdot}H_2O$, 0.15 μM $ZnSO_4{\cdot}7H_2O$, 0.16 μM $CuSO_4$, and 0.52 μM $(NH_4)_3Mo_7O_{24}{\cdot}4H_2O$, pH 5.5), and growth was continued in a greenhouse. Compositions of nutrient solutions containing different levels of supplied nitrogen were as follows: 1N, 1.25 mM NH_4NO_3; 0.6N, 0.75 mM NH_4NO_3; 0.2N, 0.25 mM NH_4NO_3; 0N, 0 mM NH_4NO_3. All nutrient solutions were changed twice per week; pH was adjusted to 5.5 every day. The temperature was maintained at 30°C day and 22°C night, and the relative humidity was 70%.

Map-based cloning of NGR5

Fine-scale mapping of *ngr5* was based on 600 F_2 plants and 1256 BC_1F_2 plants derived from a cross between the *ngr5* mutant and the *japonica* rice cultivar Lansheng (recurrent parent). Genomic DNA sequences in the candidate region were compared between 9311, Nipponbare, and Lansheng. Primer sequences used for map-based cloning and genotyping assays are given in table S7.

Transgene constructs

Wild-type *NGR5* and *ngr5* mRNA-encoding sequences (together with intron sequences and/or promoter regions lying 3 kbp upstream of the transcription start site) were amplified from 9311 and *ngr5* mutant plants, respectively. These amplified genomic DNA fragments were inserted into the *p35S::HA-nos* (*40*) and *pCAMBIA1300* (CAMBIA, www.cambia.org) vectors to respectively generate *pNGR5::NGR5*, *pNGR5::ngr5*, *pNGR5::NGR5-HA*, and *p35S::NGR5* constructs. Full-length cDNAs of *NGR5*, *GID1*, and *LC2* cDNAs were amplified from 9311 plants and inserted into *p35S::HA-nos* (*40*) or *p35::GFP-nos* (*39*–*41*) vector to respectively generate *p35S::GID1*, *p35S::LC2-HA*, *p35S::NGR5-HA*, and *p35S::NGR5-GFP* constructs. gRNA constructs required for CRISPR/Cas9-mediated generation of *GID1*, *GID2*, and *LC2* mutant alleles were made as described (*13*, *41*). The transgenic rice plants were generated by *Agrobacterium*-mediated transformation as described (*42*). Relevant primer sequences are given in table S8.

qRT-PCR analysis

Total RNAs were extracted from tiller buds of 3-week-old rice plants using the TRIzol reagent (Invitrogen) according to the manufacturer's protocol, and treated with RNase-free DNase I (Invitrogen) to remove contaminating genomic DNAs. The full-length cDNAs were then reverse-transcribed using a cDNA synthesis kit (TRANSGEN, AE311-02). Subsequent qRT-PCR processing steps were performed according to the manufacturer's instructions (TRANSGEN, AQ101), with each qRT-PCR assay being replicated at least three times with three independent RNA preparations. Rice *Actin1* gene (*OsActin1*, LOC_Os03 g50885) transcripts were used as an internal reference. Relevant primer sequences are given in table S9.

Yeast two-hybrid assays

Yeast two-hybrid screening was performed as described (*38*). The full length *NGR5* cDNA was amplified and subcloned into *pGBKT7* (Takara Bio Inc.), then transformed into yeast strain AH109. The NGR5 protein was used as a bait to screen a cDNA library prepared from equal amounts of poly(A)-containing RNA sampled from various rice tissues/organs, including tiller buds, roots, leaves, shoot apical meristem (SAM), young panicles, etc. Experimental procedures for screening and plasmid isolation were performed according to the

manufacturer's user guide. cDNAs encoding various deleted and nondeleted versions of SLR1 were amplified and then subcloned into the *pGBKT7* vector (Takara Bio Inc.). Bait and prey vectors were co-transformed into yeast strain AH109, and experimental procedures were performed according to the manufacturer's instructions (Takara Bio Inc.). Relevant primer sequences are given in table S8.

Bimolecular fluorescence complementation (BiFC) assays

As described (*13*), full-length cDNAs of *NGR5*, *LC2*, *SLR1*, *DLT*, and *MOC1* were amplified from 9311 and inserted into *pSY-735-35S-cYFP-HA* or *pSY-736-35S-nYFP-EE* vectors (YFP, yellow fluorescent protein) to generate fusion constructs. Cotransfection of constructs (e.g., nYFP-NGR5 and cYFP-LC2) into tobacco leaf epidermal cells by *Agrobacterium*-mediated infiltration enabled testing for protein-protein interaction. After 48 hours of incubation in the dark, the YFP signal was captured using a confocal microscope (Zeiss LSM710). Each BiFC assay was repeated at least three times. Relevant primer sequences are given in table S8.

Split firefly luciferase complementation (SFLC) assays

Full-length cDNAs of *GID1* and *GID2* and cDNAs encoding various deleted and nondeleted versions of *NGR5* were amplified from 9311, and then inserted into *pCAMBIA1300-35S-Cluc-RBS* or *pCAMBIA1300-35S-HA-Nluc-RBS* vectors (*39*) to generate fusion constructs. Two different vectors (e.g., nLUC-GID1 and cLUC-NGR5) enabling testing of protein-protein interaction, together with the p19 silencing plasmid, were cotransfected into tobacco leaf epidermal cells by *Agrobacterium*-mediated infiltration. After 48 hours of incubation in the dark, the injected leaves were sprayed with 1 mM luciferin (Promega, E1605) and the LUC signal was captured using a cooled CCD imaging apparatus (Berthold, LB985). Each assay was repeated at least three times. Relevant primer sequences are given in table S8.

FRET (Förster resonance energy transfer) assays

FRET assays were performed as described (*13*). Cauliflower mosaic virus (CaMV) *35S* promoter-driven fusion constructs with C-terminal tagging CFP (cyan fluorescent protein) or YFP were created to generate the donor vectors *p35S::GID1-CFP* (or *p35S::LC2-CFP*), and the acceptor vector *p35S::NGR5-YFP*. Donor and acceptor vectors, with or without *p35S::Rht-B1a* (*p35S::Rht-B1b*, or *p35S::SLR1*) vector, were cotransformed into tobacco leaf epidermis cells by *Agrobacterium*-mediated vacuum infiltration to provide the FRET measurements. Transformation with the *p35S::GID1-CFP* vector provided only the donor channel, and with the *p35S::NGR5-YFP* vector only the acceptor channel. The FRET signal was detected and photographed using a confocal microscope (Zeiss LSM710). Relevant primer sequences are given in table S8.

Western blotting and coimmunoprecipitation (Co-IP) assays

Protein extracts were electrophoretically separated by SDS-PAGE and transferred to a nitrocellulose membrane (GE Healthcare). Proteins were detected by immunoblot using the following antibodies: anti-SLR1 (ABclonal Technology), anti-HA (MBL, M180-7), anti-Ubiquitin (Abcam, ab134953), anti-GST (Santa Cruz, sc-138), anti-GFP (Abcam, ab6673), and anti-HSP90 (BGI), respectively. For Co-IP experiments, full-length *NGR5*, *LC2*, *SLR1*, *GID1*, and *GID2* cDNAs were amplified, then inserted into either the *pUC-35S-HA-RBS* or the *pUC-35S-Flag-RBS* vector as described (*13*, *39*). Rice protoplasts were transfected with 100 μg of plasmid DNA and then incubated overnight in the dark. Total protein was extracted from harvested protoplasts with a lysis buffer [50 mM HEPES (pH 7.5), 150 mM KCl, 1 mM EDTA, 0.5% Triton X-100, 1 mM DTT, proteinase inhibitor cocktail (Roche LifeScience)]. Lysates were incubated with magnetic beads conjugated with an anti-DDDDK-tag antibody (MBL, M185-11) or anti-HA-tag antibody (MBL, M180-11) at 4°C for 4 hours. The magnetic beads were then washed 5 times with TBS-T buffer [500 mM NaCl, 20 mM Tris-HCl (pH 8.0), 0.1% Tween 20] and eluted with 3×Flag peptide (Sigma-Aldrich, F4709). Immunoprecipitates were electrophoretically separated and specific proteins detected by immunoblotting with anti-HA (MBL, M180-7) or anti-DDDDK (MBL, M185-7) antibodies. Relevant primer sequences are given in table S8.

In vivo pull-down

A full-length rice *GID1* cDNA was amplified and then inserted into the *pGEX-4T-1* vector (GE Healthcare). The recombinant GST-GID1 protein was expressed in *Escherichia coli* BL21 (DE3) (Transgen, CD701-01), and then purified and immobilized on Glutathione Sepharose 4B beads (GE Healthcare, 17-0756) following the manufacturer's instructions. The beads were divided into four equal aliquots and incubated with the same amount of NGR5-HA (or NGR5-Flag) protein lysate, together with His-SLR1 or with different concentrations of GA_3 (0, 2, 5, 10 μM) and/or MG132 (50 μM) for 2 hours at 4°C. The beads were subsequently washed five times with TBS-T buffer, followed by elution with 50 μl of elution buffer (50 mM Tris-HCl, 10 mM reduced glutathione, pH 8.0). Supernatants were resolved by 12% SDS-PAGE and subjected to immunoblotting using anti-GST (Santa Cruz, sc-138) and anti-HA (MBL, M180-7) antibodies. Relevant primer sequences are given in table S8.

EMSA assays

EMSA assays were performed as described (*39*). A full-length *NGR5* cDNA was amplified and inserted into the *pGEX-4T-1* vector (GE Healthcare). Recombinant GST-NGR5 protein was expressed in *E. coli* BL21 (DE3) strain and purified using Glutathione Sepharose 4B (GE Healthcare, 17-0756) following the manufacturer's instructions. DNA probes (D5 fragment for the *D14* gene, S3 fragment for the *OsSPL14* gene) were amplified and labeled using a biotin label kit (Biosune). DNA gel shift assays were performed using the LightShift Chemiluminescent EMSA kit (Thermo Fisher Scientific, 20148). Relevant primer sequences are given in table S10.

Cell-free protein degradation assays

Three-week-old NJ6-*gid1-c1* and NJ6-*gid2-c1* seedlings (together with NJ6) were harvested and ground into a fine powder in liquid nitrogen. Lysates were subsequently extracted with lysis buffer [25 mM Tris-HCl (pH 7.5), 10 mM NaCl, 10 mM $MgCl_2$, 4 mM PMSF, 5 mM DTT, and 10 mM ATP] as described (*43*); total protein extracts were adjusted to be at equal concentration in the lysis buffer for each assay. Rice cell lysates (200 μl) were incubated with 100 ng of purified GST-NGR5 (or His-NGR5) fusion protein in the presence or absence of the recombinant Rht-B1b-Flag, Rht-B1a-Flag, SLR1-Flag, or His-SLR1 proteins. Proteins were extracted from lysates that had or had not been exposed to treatments with 100 μM GA_3 and/or 100 μM MG132 for a series of incubation times and then subjected to SDS-PAGE and Western blotting using an anti-GST antibody (Santa Cruz, sc-138). HSP90 was used as a loading control.

In vitro protein ubiquitination assays

Full-length *GID2* cDNA was amplified and inserted into *PUC-35S-flag-RBS* vector (*39*). Rice protoplasts were transfected with 100 μg of plasmid and incubated for 24 hours. Total protein was extracted from harvested protoplasts in the lysis buffer [50 mM HEPES (pH 7.5), 150 mM KCl, 1 mM EDTA, 0.5% Triton X-100, 1 mM DTT, and proteinase inhibitor cocktail (Roche LifeScience)]. Lysates were incubated with agarose-conjugated anti-Flag antibodies (Sigma-Aldrich, A2220) at 4°C for 2 hours, rinsed 6 times in the PBS-T buffer, and then eluted with 3×Flag peptide (Sigma-Aldrich). Purified GID2-Flag proteins were used for in vitro ubiquitination assays as described (*44*). Crude extracts containing recombinant GST-NGR5, purified E3 (GID2-Flag), 6×His-tagged Ubiquitin (Ub), E1 and E2 (Ubiquitinylation kit; Enzo Life Science, BML-UW9920-0001) were used. Buffer at a final concentration of 50 mM Tris-HCl (pH 7.4), 5 mM $MgCl_2$, and 2 mM ATP was also added to the system. The reactions were incubated at 30°C for 2 hours,

and terminated by adding SDS sample buffer with β-mercaptoethanol. Reaction products were separated with 12% SDS-PAGE and subjected to immunoblotting using anti-ubiquitin antibody (Abcam, ab134953) and anti-GST antibody (Santa Cruz, sc-138). Relevant primer sequences are given in table S8.

ChIP-PCR assay

ChIP assays were performed as described (*13*). A 2-g sample of 2-week-old rice plants was collected and immediately fixed with 1% (v/v) formaldehyde under vacuum for 15 min at 25°C, and then homogenized in liquid nitrogen. After the nuclei were isolated and lysed, the chromatin was ultrasonically fragmented on ice to an average size of 500 bp. Immunoprecipitations were performed with an anti-HA antibody (Santa Cruz, sc-7932x) and an anti-H3K27me3 antibody (Millipore, 07-449) overnight at 4°C. At the same time, an equal volume of the supernatant was prepared without any antibody as a mock sample. The bound DNA fragments were then reversely released and amplified by real-time quantitative PCR. Relevant primer sequences are listed in table S11.

RNA-seq

Total RNAs were extracted from tiller buds of 3-week-old 9311 plants treated with and without gibberellin and *ngr5* mutants grown in high N (1.25 mM NH_4NO_3) supply conditions using the TRIzol reagent (Invitrogen) according to the manufacturer's instructions. Libraries were constructed and sequenced using the BGISEQ-500 sequencer. Raw sequencing reads were cleaned by removing adaptor sequences, reads containing poly-N sequences, and low-quality reads, and clean reads were then mapped to the Nipponbare reference genome as described (*13*).

ChIP-seq

ChIP-Seq analysis was performed as described (*13*). Approximately 2 g of 2-week-old transgenic plants carrying the *p35S::LC2-HA* and *pNGR5::NGR5-HA* constructs grown in high N (1N, 1.25 mM NH_4NO_3) supply conditions, and of *ngr5* and wild-type plants grown in low (0.2N, 0.25 mM NH_4NO_3) or high nitrogen (1N, 1.25 mM NH_4NO_3) supply conditions with or without 100 μM GA_3 (Sigma-Aldrich, G1025) and 10 μM PAC (Sigma-Aldrich, 19847) treatments, were fixed with 1% (v/v) formaldehyde under vacuum for 15 min at 25°C, and then homogenized in liquid nitrogen. After cell lysis and nucleic acid isolation, cross-linked chromatin fibers were ultrasonically fragmented into fragments of an average size of 500 bp. Immunoprecipitations were performed with anti-HA antibodies (Santa Cruz, sc-7932) and anti-H3K27me3 antibodies (Millipore, 07-449) overnight at 4°C. The precipitated DNA was recovered by centrifugation (13,000*g*, 5 min, 25°C) and dissolved in sterile distilled water. Illumina sequencing libraries were constructed according to the manufacturer's instructions, and then sequenced on the BGISEQ-500 platform. Sequencing reads were mapped to the reference genome as described (*13*). The precipitated DNA samples also served as template for quantitative real-time PCR. Relevant primer sequences are given in table S11.

Processing of ChIP- and RNA-sequencing data

Sequencing reads were cleaned with Trimmomatic (version 0.36) (*45*) and Sickle, including elimination of bases with low-quality scores (< 25) and irregular GC contents, as well as removal of sequencing adapters and short reads. The remaining clean reads were mapped to the genome of japonica rice (MSU7.0 release) with the Burrows-Wheeler Aligner-backtrack (version 0.7.16a-r1181) (*46*) for ChIP-sequencing data and HISAT2 2.1.0 (*47*) for RNA-seq data. MACS (version 1.3.7) (*48*) was used to identify read-enriched regions (peaks) of ChIP-sequencing databased on the following combined criteria: P value < 0.00001 and fold-change > 32. Target genes were defined as genes with a peak within or near the gene body (±2 kb). DESeq (*49*) was applied to determine the significance of the differential expression between samples with the combined criteria: fold change > 2 and adj. P < 0.05.

Gene set enrichment analysis

To determine the enrichment of H3K27me3 targets in *NGR5*-regulated genes (i.e., differentially expressed genes in ngr5), we performed gene set enrichment analysis (GSEA), which is a robust computational method that determines whether an a priori gene set shows statistically significant and concordant differences between two samples (*50*). Briefly, *NGR5* regulated genes were ranked by the quantitative expression change in *ngr5*, followed by calculation of the fraction of regulated genes that are targeted by H3K27me3. The enrichment score is normalized by the size of the gene set (NES). P value is estimated by permutating genes.

Statistical analysis

Data were statistically analyzed and multiple comparisons were made using Duncan's multiple range test as described (*13*). P values of less than 0.05 were considered to indicate statistical significance. Statistical calculations were performed using Microsoft Excel 2010.

REFERENCES AND NOTES

1. G. S. Khush, Green revolution: Preparing for the 21st century. *Genome* **42**, 646–655 (1999). doi: 10.1139/g99-044; pmid: 10464789
2. P. L. Pingali, Green revolution: Impacts, limits, and the path ahead. *Proc. Natl. Acad. Sci. U.S.A.* **109**, 12302–12308 (2012). doi: 10.1073/pnas.0912953109; pmid: 22826253
3. R. E. Evenson, D. Gollin, Assessing the impact of the green revolution, 1960 to 2000. *Science* **300**, 758–762 (2003). doi: 10.1126/science.1078710; pmid: 12730592
4. P. Hedden, The genes of the Green Revolution. *Trends Genet.* **19**, 5–9 (2003). doi: 10.1016/S0168-9525(02)00009-4; pmid: 12493241
5. J. Peng *et al.*, 'Green revolution' genes encode mutant gibberellin response modulators. *Nature* **400**, 256–261 (1999). doi: 10.1038/22307; pmid: 10421366
6. C. Zhang, L. Gao, J. Sun, J. Jia, Z. Ren, Haplotype variation of Green Revolution gene *Rht-D1* during wheat domestication and improvement. *J. Integr. Plant Biol.* **56**, 774–780 (2014). doi: 10.1111/jipb.12197; pmid: 24645900
7. A. Sasaki *et al.*, A mutant gibberellin-synthesis gene in rice. *Nature* **416**, 701–702 (2002). doi: 10.1038/416701a; pmid: 11961544
8. W. Spielmeyer, M. H. Ellis, P. M. Chandler, Semidwarf (*sd-1*), "green revolution" rice, contains a defective gibberellin 20-oxidase gene. *Proc. Natl. Acad. Sci. U.S.A.* **99**, 9043–9048 (2002). doi: 10.1073/pnas.132266399; pmid: 12077303
9. N. P. Harberd, E. Belfield, Y. Yasumura, The angiosperm gibberellin-GID1-DELLA growth regulatory mechanism: How an "inhibitor of an inhibitor" enables flexible response to fluctuating environments. *Plant Cell* **21**, 1328–1339 (2009). doi: 10.1105/tpc.109.066969; pmid: 19470587
10. H. Xu, Q. Liu, T. Yao, X. Fu, Shedding light on integrative GA signaling. *Curr. Opin. Plant Biol.* **21**, 89–95 (2014). doi: 10.1016/j.pbi.2014.06.010; pmid: 25061896
11. H. Itoh, M. Ueguchi-Tanaka, Y. Sato, M. Ashikari, M. Matsuoka, The gibberellin signaling pathway is regulated by the appearance and disappearance of SLENDER RICE1 in nuclei. *Plant Cell* **14**, 57–70 (2002). doi: 10.1105/tpc.010319; pmid: 11826299
12. K. Asano *et al.*, Artificial selection for a green revolution gene during *japonica* rice domestication. *Proc. Natl. Acad. Sci. U.S.A.* **108**, 11034–11039 (2011). doi: 10.1073/pnas.1019490108; pmid: 21646530
13. S. Li *et al.*, Modulating plant growth-metabolism coordination for sustainable agriculture. *Nature* **560**, 595–600 (2018). doi: 10.1038/s41586-018-0415-5; pmid: 30111841
14. H. Sun *et al.*, Heterotrimeric G proteins regulate nitrogen-use efficiency in rice. *Nat. Genet.* **46**, 652–656 (2014). doi: 10.1038/ng.2958; pmid: 24777451
15. G. W. Wu, L. T. Wilson, A. M. McClung, Contribution of rice tillers to dry matter accumulation and yield. *Agron. J.* **90**, 317–323 (1998). doi: 10.2134/agronj1998.00021962009000030001x
16. M. Ueguchi-Tanaka *et al.*, GIBBERELLIN INSENSITIVE DWARF1 encodes a soluble receptor for gibberellin. *Nature* **437**, 693–698 (2005). doi: 10.1038/nature04028; pmid: 16193045
17. Z. Liao *et al.*, SLR1 inhibits MOC1 degradation to coordinate tiller number and plant height in rice. *Nat. Commun.* **10**, 2738 (2019). doi: 10.1038/s41467-019-10667-2; pmid: 31227696
18. K. Aya *et al.*, A novel AP2-type transcription factor, SMALL ORGAN SIZE1, controls organ size downstream of an auxin signaling pathway. *Plant Cell Physiol.* **55**, 897–912 (2014). doi: 10.1093/pcp/pcu023; pmid: 24486766
19. K. Hirano *et al.*, SMALL ORGAN SIZE 1 and SMALL ORGAN SIZE 2/DWARF AND LOW-TILLERING form a complex to integrate auxin and brassinosteroid signaling in rice. *Mol. Plant* **10**, 590–604 (2017). doi: 10.1016/j.molp.2016.12.013; pmid: 28069545
20. S. Qiao *et al.*, The RLA1/SMOS1 transcription factor functions with OsBZR1 to regulate brassinosteroid signaling and rice architecture. *Plant Cell* **29**, 292–309 (2017). doi: 10.1105/tpc.16.00611; pmid: 28100707
21. R. Yao *et al.*, DWARF14 is a non-canonical hormone receptor for strigolactone. *Nature* **536**, 469–473 (2016). doi: 10.1038/nature19073; pmid: 27479325
22. L. Jiang *et al.*, DWARF 53 acts as a repressor of strigolactone signalling in rice. *Nature* **504**, 401–405 (2013). doi: 10.1038/nature12870; pmid: 24336200
23. F. Zhou *et al.*, D14-SCF(D3)-dependent degradation of D53 regulates strigolactone signalling. *Nature* **504**, 406–410 (2013). doi: 10.1038/nature12878; pmid: 24336215
24. S. Ishikawa *et al.*, Suppression of tiller bud activity in tillering dwarf mutants of rice. *Plant Cell Physiol.* **46**, 79–86 (2005). doi: 10.1093/pcp/pci022; pmid: 15659436
25. T. Takeda *et al.*, The OsTB1 gene negatively regulates lateral branching in rice. *Plant J.* **33**, 513–520 (2003). doi: 10.1046/j.1365-313X.2003.01648.x; pmid: 12581309
26. Y. Jiao *et al.*, Regulation of OsSPL14 by OsmiR156 defines ideal plant architecture in rice. *Nat. Genet.* **42**, 541–544 (2010). doi: 10.1038/ng.591; pmid: 20495565
27. K. Miura *et al.*, OsSPL14 promotes panicle branching and higher grain productivity in rice. *Nat. Genet.* **42**, 545–549 (2010). doi: 10.1038/ng.592; pmid: 20495564

28. S. Wang *et al*., Non-canonical regulation of SPL transcription factors by a human OTUB1-like deubiquitinase defines a new plant type rice associated with higher grain yield. *Cell Res.* **27**, 1142–1156 (2017). doi: 10.1038/cr.2017.98; pmid: 28776570
29. T. Arite *et al*., d14, a strigolactone-insensitive mutant of rice, shows an accelerated outgrowth of tillers. *Plant Cell Physiol.* **50**, 1416–1424 (2009). doi: 10.1093/pcp/pcp091; pmid: 19542179
30. J. Wang, J. Hu, Q. Qian, H. W. Xue, LC2 and OsVIL2 promote rice flowering by photoperoid-induced epigenetic silencing of *OsLF*. *Mol. Plant* **6**, 514–527 (2013). doi: 10.1093/mp/sss096; pmid: 22973062
31. A. Sasaki *et al*., Accumulation of phosphorylated repressor for gibberellin signaling in an F-box mutant. *Science* **299**, 1896–1898 (2003). doi: 10.1126/science.1081077; pmid: 12649483
32. X. Fu *et al*., The Arabidopsis mutant sleepy1gar2-1 protein promotes plant growth by increasing the affinity of the SCF^{SLY1} E3 ubiquitin ligase for DELLA protein substrates. *Plant Cell* **16**, 1406–1418 (2004). doi: 10.1105/tpc.021386; pmid: 15161962
33. K. Murase, Y. Hirano, T. P. Sun, T. Hakoshima, Gibberellin-induced DELLA recognition by the gibberellin receptor GID1. *Nature* **456**, 459–463 (2008). doi: 10.1038/nature07519; pmid: 19037309
34. A. Shimada *et al*., Structural basis for gibberellin recognition by its receptor GID1. *Nature* **456**, 520–523 (2008). doi: 10.1038/nature07546; pmid: 19037316
35. Z. Wu *et al*., Characterization of a new semi-dominant dwarf allele of SLR1 and its potential application in hybrid rice breeding. *J. Exp. Bot.* **69**, 4703–4713 (2018). doi: 10.1093/jxb/ery243; pmid: 29955878
36. H. Tong *et al*., DWARF AND LOW-TILLERING, a new member of the GRAS family, plays positive roles in brassinosteroid signaling in rice. *Plant J.* **58**, 803–816 (2009). doi: 10.1111/j.1365-313X.2009.03825.x; pmid: 19220793
37. W. Wang *et al*., Genomic variation in 3,010 diverse accessions of Asian cultivated rice. *Nature* **557**, 43–49 (2018). doi: 10.1038/s41586-018-0063-9; pmid: 29695866
38. S. Wang *et al*., The *OsSPL16-GW7* regulatory module determines grain shape and simultaneously improves rice yield and grain quality. *Nat. Genet.* **47**, 949–954 (2015). doi: 10.1038/ng.3352; pmid: 26147620
39. Q. Liu *et al*., G-protein βγ subunits determine grain size through interaction with MADS-domain transcription factors in rice. *Nat. Commun.* **9**, 852 (2018). doi: 10.1038/s41467-018-03047-9; pmid: 29487282
40. S. Wang *et al*., Control of grain size, shape and quality by OsSPL16 in rice. *Nat. Genet.* **44**, 950–954 (2012). doi: 10.1038/ng.2327; pmid: 22729225
41. X. Ma *et al*., A robust CRISPR/Cas9 system for convenient, high-efficiency multiplex genome editing in monocot and dicot plants. *Mol. Plant* **8**, 1274–1284 (2015). doi: 10.1016/j.molp.2015.04.007; pmid: 25917172
42. X. Huang *et al*., Natural variation at the *DEP1* locus enhances grain yield in rice. *Nat. Genet.* **41**, 494–497 (2009). doi: 10.1038/ng.352; pmid: 19305410
43. F. Wang *et al*., Biochemical insights on degradation of Arabidopsis DELLA proteins gained from a cell-free assay system. *Plant Cell* **21**, 2378–2390 (2009). doi: 10.1105/tpc.108.065433; pmid: 19717618
44. Q. Zhao *et al*., A plant-specific in vitro ubiquitination analysis system. *Plant J.* **74**, 524–533 (2013). doi: 10.1111/tpj.12127; pmid: 24695404
45. A. M. Bolger, M. Lohse, B. Usadel, Trimmomatic: A flexible trimmer for Illumina sequence data. *Bioinformatics* **30**, 2114–2120 (2014). doi: 10.1093/bioinformatics/btu170; pmid: 24695404
46. H. Li, R. Durbin, Fast and accurate short read alignment with Burrows-Wheeler transform. *Bioinformatics* **25**, 1754–1760 (2009). doi: 10.1093/bioinformatics/btp324; pmid: 19451168
47. D. Kim, B. Langmead, S. L. Salzberg, HISAT: A fast spliced aligner with low memory requirements. *Nat. Methods* **12**, 357–360 (2015). doi: 10.1038/nmeth.3317; pmid: 25751142
48. Y. Zhang *et al*., Model-based analysis of ChIP-Seq (MACS). *Genome Biol.* **9**, R137 (2008). doi: 10.1186/gb-2008-9-9-r137; pmid: 18798982
49. S. Anders, W. Huber, Differential expression analysis for sequence count data. *Genome Biol.* **11**, R106 (2010). doi: 10.1186/gb-2010-11-10-r106; pmid: 20979621
50. A. Subramanian *et al*., Gene set enrichment analysis: A knowledge-based approach for interpreting genome-wide expression profiles. *Proc. Natl. Acad. Sci. U.S.A.* **102**, 15545–15550 (2005). doi: 10.1073/pnas.0506580102; pmid: 16199517

ACKNOWLEDGMENTS

We thank C. Sun for providing the CSSLs, Q. Qian for providing *d14*, Z. Cheng for providing *Slr1-d6*, and M. Matsuoka for critical comments on the manuscript. **Funding:** Supported by the National Key Research and Development Program of China (2016YFD0100401, 2016YFD0100706), the National Key Program on Transgenic Research from the Ministry of Agriculture of China (2016ZX08009-001, 2016ZX08009-003), the National Natural Science Foundation of China (31830082, 31921005, 91935301, 31970304), the Strategic Priority Research Program of the Chinese Academy of Sciences (XDB27010000), and the Biological and Biotechnological Sciences Research Council (UK) "Newton Fund" Rice Research Initiative grant BB/N013611/1. **Author contributions:** K.W. performed most of the experiments; K.W., B.L., and Y.W. conducted the *NGR5* mutation screening; S.W. and K.W. performed map-based cloning and genetic complementation; K.W., W.S., J.C., and J.Z. constructed NILs and mutant plants; K.W., S.W., S.L., and Q.L. characterized the phenotypes of transgenic plants; W.S., X.W., and K.W. conducted protein-protein interactions; K.W., Y.Z., and J.W. performed field experiments; M.W., K.W., and Y.J.Z. performed analysis of ChIP-seq and RNA-seq; Y.W. and J.Y. performed haplotype analysis; K.W., N.P.H., and X.F. designed experiments; N.P.H. and X.F. wrote the manuscript; and all authors discussed and commented on the manuscript. **Competing interests:** The authors declare no competing interests. **Data and materials availability:** The raw sequence data reported in this paper have been deposited in the Genome Sequence Archive in BIG Data Center of CRA002108 that are publicly accessible at https://bigd.big.ac.cn/gsa. Requests for materials should be addressed to X.F. All of the data pertaining to the work are contained within the figures and supplementary materials.

SUPPLEMENTARY MATERIALS

science.sciencemag.org/content/367/6478/eaaz2046/suppl/DC1
Materials and Methods
Figs. S1 to S15
Tables S1 to S11

20 August 2019; accepted 18 December 2019
10.1126/science.aaz2046

Science

Enhanced sustainable green revolution yield via nitrogen-responsive chromatin modulation in rice

Kun Wu, Shuansuo Wang, Wenzhen Song, Jianqing Zhang, Yun Wang, Qian Liu, Jianping Yu, Yafeng Ye, Shan Li, Jianfeng Chen, Ying Zhao, Jing Wang, Xiaokang Wu, Meiyue Wang, Yijing Zhang, Binmei Liu, Yuejin Wu, Nicholas P. Harberd and Xiangdong Fu

Science **367** (6478), eaaz2046.
DOI: 10.1126/science.aaz2046

Decoupling tillering and fertilization

For rice as an agricultural crop, more tillers, or branches that carry grains, are desired, as is less demand for nitrogen fertilization. Unfortunately, for many rice varieties, the number of tillers depends on the amount of nitrogen fertilization. Wu *et al.* now show that nitrogen status affects chromatin function through modification of histones, a process in which the transcription factor NGR5 recruits polycomb repressive complex 2 to target genes. Some of these genes regulate tillering, such that with more nitrogen, the plants develop more tillers. NGR5 is regulated by proteasomal destruction and mediates hormone signaling. An increase in NGR5 levels can drive increases in rice tillering and yield without requiring increases in nitrogen-rich fertilizer.

Science, this issue p. eaaz2046